Progress toward Système International d'Unités traceable force metrology for nanomechanics

Jon R. Pratt, Douglas T. Smith, David B. Newell, John A. Kramar, and Eric Whitenton
National Institute of Standards and Technology, Gaithersburg, Maryland 20899

(Received 16 June 2003; accepted 28 October 2003)

Recent experiments with the National Institute of Standards and Technology (NIST) Electrostatic Force Balance (EFB) have achieved agreement between an electrostatic force and a gravitational force of 10^{-5} N to within a few hundred pN/μN. This result suggests that a force derived from measurements of length, capacitance, and voltage provides a viable small force standard consistent with the Système International d'Unités. In this paper, we have measured the force sensitivity of a piezoresistive microcantilever by directly probing the NIST EFB. These measurements were linear and repeatable at a relative standard uncertainty of 0.8%. We then used the calibrated cantilever as a secondary force standard to transfer the unit of force to an optical lever–based sensor mounted in an atomic force microscope. This experiment was perhaps the first ever force calibration of an atomic force microscope to preserve an unbroken traceability chain to appropriate national standards. We estimate the relative standard uncertainty of the force sensitivity at 5%, but caution that a simple model of the contact mechanics suggests errors may arise due to friction.

I. INTRODUCTION

Commercial and custom mechanical test instruments, including instrumented indentation machines and atomic force microscopes, have recently been developed with displacement resolutions extending into the nanometer level and with force detection capabilities extending to the nanonewton regime. These devices are used for studying micromechanical material properties such as hardness and modulus,[1] fatigue and fracture of thin films,[2,3] adhesion of ultra-thin films,[4] and even for the measurement of covalent bond forces.[5] This field of experimental mechanics, or nanomechanics as it is being called, is of ever-increasing importance in the development of new materials and products. In Fig. 1, we attempt to capture a sense of the tremendous scope of the forces, phenomena, and instruments encountered.

As miniaturization trends continue in advanced technology industries, for example in the manufacture of microelectronics, photonics, data storage devices, and microelectromechanical systems (MEMS), it is increasingly necessary to rely on nanoscale measurements for the control of manufacturing processes, the evaluation of device performance, and the characterization of material behavior. Correspondingly, a desire for accurate, traceable, nanoscale length and force measurement is emerging within the International Organization for Standardization (ISO) task groups and American Society for Testing and Materials committees. Of particular interest to the audience of this *Journal of Materials Research* focus issue on instrumented indentation are the efforts of these groups to develop instrumented indentation standards.[6]

At a basic level, instrumented indentation requires measurement of two units that are well defined within the Système International d'Unités (SI): a length and a force. The ability to realize a change in length of 1 nm using the wavelength of light is challenging but achievable within the realm of established metrology techniques based on subdividing interference fringes (although length becomes of limited absolute accuracy at this level, with the best interferometer at the National Institute of Standards and Technology (NIST) having achieved resolution accuracy of just less than 10 picometer (pm),[7] or approximately 1% of a nanometer). The situation in force is even worse: no methods for establishing force measurement traceability at levels below 10^{-5} N are currently available. It is within this context that NIST is seeking to develop competency in the realization and measurement of microforces by creating a facility and instruments capable of providing a viable primary force standard below 10^{-5} N; the goal being to realize force in this range at a relative uncertainty of as little as 10 pN/μN. This new project complements a body of existing work at NIST to develop standards and methods for the instrumented indentation community, with the two combining to provide a metrological basis for manufacturers seeking traceable characterization of thin film mechanical properties.

In what follows, we briefly review the working principles of the NIST electrostatic force balance (EFB) and

Downloaded from http:/www.cambridge.org/core. the NIST Virtual Library (NVL), on 27 Sep 2016 at 19:16:31, subject to the Cambridge Core terms of use, available at http:/www.cambridge.org/core/terms. http://dx.doi.org/10.1557/jmr.2004.19.1.366

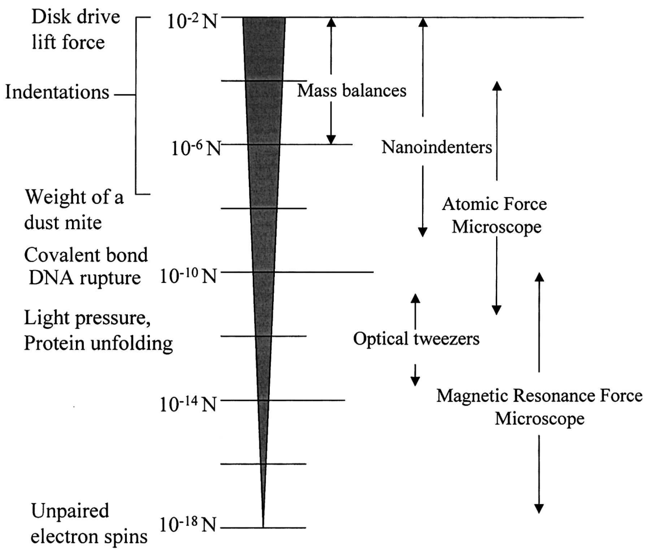

FIG. 1. Relative magnitude of small force phenomena and instruments used for their measurement

describe how it can be used to provide a realization of small force, potentially accurate enough to serve as a primary standard of force for calibrating probe-style force sensors. In fact, we advocate the EFB as a viable standard for the top of the metrology hierarchy for small force and suggest a methodology for calibrating probe force sensors against it. Once calibrated in this fashion, these small force sensors can directly be used as the sensing element in force probe instruments to achieve calibrated force measurements or they can serve as calibration specimens, or secondary force standards, that can be probed by other instruments needing calibration.

To illuminate these concepts, we report the results of an experiment to calibrate the force sensitivity of a commercially available piezoresistive cantilever. This device was selected as an example of a candidate probe sensor whose calibration might prove useful to atomic force microscope–style force probe instruments. The results reported in this paper show repeatability in the determination of its force sensitivity below a percent for a specific contact condition. However, we also argue from basic mechanics that these results can be subject to errors due to the friction produced by the contact conditions. Finally, having demonstrated the ability to calibrate this piezoresistive cantilever as a "load cell," the device is used as a secondary force standard to calibrate an atomic force microscope. This entails operating the atomic force microscope as a force probe, pressing its cantilever against the calibrated piezoresistive sensor in a single-axis scan normal to the specimen stage.

II. SI FORCE REALIZATION

The most common approach to force realization, and the one universally accepted as a primary standard of force, is a calibrated mass in a known gravitational field, or deadweight force. Unfortunately, the precision of deadweight force is linked to mass and decreases as the masses are subdivided to achieve smaller forces. The smallest calibrated mass available from NIST is 0.5 mg (~5 μN) and has a relative uncertainty of a few tenths of a μg/mg. In principle, smaller masses could be calibrated, but they would be difficult to handle, and the trend is for the relative uncertainty to increase in inverse proportion to the decrease in mass.[8] If this trend continues, the uncertainty will likely reach the same magnitude as the force at a dead weight producing 1 nN.

Force is a derived unit within the SI and can in principle be realized using whatever physics are convenient, provided the physics can be expressed in terms of measured quantities that are themselves expressed in terms of some combination of the SI base units. Conceptually, forces can be realized in this range using the SI unit of length in combination with the electrical units defined in the SI and linked to the Josephson and quantized Hall effects. This realization can be done using electromagnetic forces (e.g., the NIST Watt balance experiment[9]) or using electrostatic forces,[10] although such energy balance experiments were originally conceived to define electrical units in terms of SI mechanical quantities. We have chosen to realize an electrostatic force rather than an electromagnetic force because the required metrology seems somewhat simpler to execute, and the forces generated, although generally less than those feasible electromagnetically, are appropriate for the force range of interest. Also, electrostatic force generation is common in MEMS, and the demonstration that these forces can be calibrated from electrical and length measurements could prove beneficial.

A. Electrostatic force balance

The mechanical work required to change the position of two electrodes with respect to one another in a one-dimensional capacitor (only the overlap or separation can vary) while maintaining constant voltage is:

$$\mathrm{d}W = F \cdot \mathrm{d}z = \tfrac{1}{2}U^2\,\mathrm{d}C \quad , \qquad (1)$$

where dW is the change in energy (mechanical work), F is the force, dz is the change in the overlap or separation of the electrodes, U is the electric potential across the capacitor, and dC is the change in capacitance. Thus, force can be realized from electrical units by measuring U and the capacitance gradient dC/dz, or

$$F = \tfrac{1}{2}U^2 \frac{\mathrm{d}C}{\mathrm{d}z} \quad . \qquad (2)$$

This is of course an idealized one-dimensional approximation of a physical system that will in truth be multidimensional and exist within a host of external fields and

Downloaded from http:/www.cambridge.org/core. the NIST Virtual Library (NVL), on 27 Sep 2016 at 19:16:31, subject to the Cambridge Core terms of use, available at http:/www.cambridge.org/core/terms. http://dx.doi.org/10.1557/jmr.2004.19.1.366

stray electrical charges. The goal is to assemble a system that reproduces this idealization as closely as possible through the use of proper constraints on the geometry and suspension of the resulting electrodes along with effective shielding from perturbing fields and charges. Also, in developing a prototype, it has been advantageous to validate this electrostatic force realization against deadweight force, at least in the higher range where the uncertainty achievable mechanically is still competitive.

In consideration of these factors, we have designed our force generator to operate along a vertical axis (z direction) defined by the gravitational normal as part of an electromechanical null balance shown in Fig. 2. Observe that the electrodes consist of a pair of nested, coaxial cylinders. The outer cylinder is fixed while the inner cylinder is allowed to translate along the z axis, varying the degree of overlap. The portion of the inner cylinder outside the fixed electrode is shielded using a guard ring. The capacitance of this geometry is in principle a linear function of the overlap of the two cylinders. In fact, for a perfectly coaxial arrangement, the resulting electrical force is directed solely along the z axis because the in-plane forces cancel one another. To define this axis of symmetry, we use a flexure translation stage. The flexure translation stage, or balance suspension system, is essentially a weak leaf spring designed to produce rectilinear motion, preventing the inner cylinder from rotating about the x, y, or z axis or from translating in the x or y directions. Deviations from a coaxial alignment cause the capacitance to vary in a nonlinear fashion with overlap and give rise to off-axis forces.

Recent results with this instrument,[11,12] referred to as the NIST EFB, demonstrated a relative standard difference of a few hundred pN/μN in the comparison of gravitational and electrostatic forces ranging between 10 μN and 100 μN. This result indicates that the electrostatic force can be constrained and measured in a fashion consistent with the SI, with accuracy sufficient to warrant consideration as a primary standard of force in this regime. The experiment consisted of operating the force generator as a null displacement force balance, where the voltage potential between the concentric cylinders was controlled to maintain a balance of forces acting on the flexure translation stage. The electric potential required to maintain the null position of the electrodes with respect to one another when a load was applied was interpreted as an SI force from previous measurements of the capacitance gradient. The gradient was obtained by displacing the moving electrode while recording the resulting change in displacement and capacitance. The measurement methods are traceable: an interferometer for displacement and a calibrated ac bridge for capacitance. It is very important to recognize that this experiment compares two different approaches to realizing the same SI force, and that this comparison is used to insure that a systematic error is not being made in the realization of either test force. Discrepancies between deadweight and electrostatic test forces indicate problems with alignment of the electrostatic force generator and gravity or the presence of other possible confounding forces arising from the dead weight interacting with the balance and environment, or vice versa. For instance, a balance calibration can be biased due to interactions of the dead weight with the environment, as was the case in early experiments, where charging of the dead weight caused it to be attracted to the automated lift used to place weights on and off the balance.

At present, the resolution of the prototype balance is of the order 10^{-8} N due to limits on the resolution of null using an interferometer to detect the deflection of the comparatively stiff balance suspension (approximately 10 nm and 13.4 N/m, respectively). The electrodes of the EFB, in principle, can easily produce test forces of any magnitude between 5×10^{-10} N and 2×10^{-4} N with a relative uncertainty of less than a part in 10^4. To take advantage of these accurate, traceable small forces, a new suspension system has been designed[13] to interface between the electrodes and test artifacts, and plans have been made to move the entire system into a vacuum chamber. The new suspension system has demonstrated the ability to produce an equivalent spring constant below 0.05 N/m using a stiffness compensation scheme. The mechanism also makes use of a counter-balanced parallelogram linkage, so the center of gravity may be located on the central pivot axis. This helps minimize the sensitivity to seismic disturbances. The move to vacuum will eliminate variations in the index of refraction that

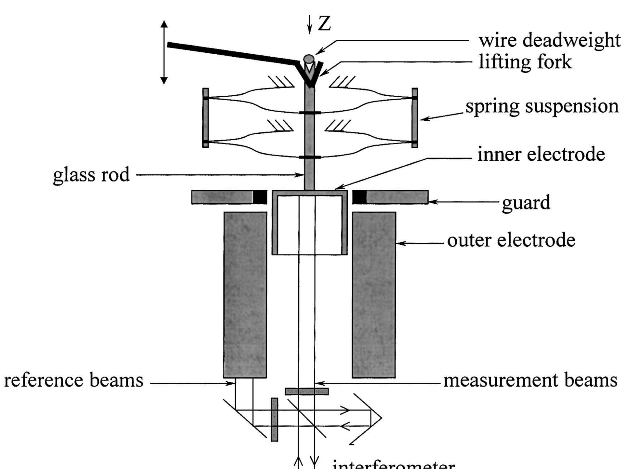

FIG. 2. The prototype electrostatic force balance. Inner cylindrical electrode of 15-mm diameter is suspended from a compound parallelogram leaf spring made of 50-μm-thick CuBe producing a single axis spring of stiffness 13.4 N/m. Deflections are measured using a double-pass Michelson interferometer and nulled using a feedback servo to apply voltage to the outer cylinder. Electrode gap is nominally 0.5 mm and overlap is nominally 5 mm.

Downloaded from http://www.cambridge.org/core. the NIST Virtual Library (NVL), on 27 Sep 2016 at 19:16:31, subject to the Cambridge Core terms of use, available at http://www.cambridge.org/core/terms. http://dx.doi.org/10.1557/jmr.2004.19.1.366

affect both the capacitance and displacement metrology, eliminate air currents and airborne acoustic vibrations that perturb the balance, and will increase the breakdown potential, extending the useful range of the balance. A range from 10 pN to 1 mN is expected due to these combined improvements.

If piconewton-level resolution is obtained, we hope to explore optical and molecular forces as alternate primary and possible intrinsic standards of force. The pressure exerted by light can be computed from determinations of the incident optical power and reflectivity using the speed of light. These measurements can be made independently using SI traceable procedures. Such an alternative SI force could be used to verify the low-range accuracy of the balance system. Observe in Fig. 1 that most covalent bonds have strengths of a few nanonewtons. The next-generation balance should enable the measurement of such forces with percent-level accuracy. It may be possible in the future to speak of intrinsic standards of force based on bond rupture strengths verified using measurements with the EFB.

The EFB is anticipated to provide a very accurate realization of force that can be used as a primary standard. It does, however, work at a slow measurement frequency (limited mechanical bandwidth) and is not a practical standard for industrial use. Eventually, it is also our purpose to evaluate transfer artifacts (i.e., calibrated load cells or force generators), through which we can disseminate this realized force to users in industry and academia. It is hoped that devices can be found that will be accurate, robust, and of suitable bandwidth. This subject forms the focus of the remainder of this paper.

III. SI FORCE DISSEMINATION: FORCE SENSORS AS TRANSFER ARTIFACTS

The typical macroscopic force transfer artifact is a high-quality strain-gauge load cell capable of reproducing changes of load within its operating range with accuracy of the order a few N/MN. At the level of micro- and, perhaps, nanonewton forces, we would like to transfer the unit of force with a more modest accuracy of a few tenths of a percent. This is the accuracy sought in draft measurement standards for instrumented indentation[6] and is representative of the growing metrology needs in the measurement of small force.

The notion of transferring the SI unit of force through an artifact is well developed at the macroscale (e.g., ASTM E74-00a) and is characterized by two fundamental approaches. As an example of the first approach, consider a typical loading apparatus, such as a materials testing machine, that is equipped with a load cell to measure the magnitude of the tensile or compressive forces that it applies along its loading axis. This load cell can be removed and calibrated against a primary standard of force, such as a deadweight-loading machine, or deadweight loads can directly be applied to the sensor in situ. In this fashion, the unit of force is disseminated to the materials testing machine via calibration of its load cell directly against a primary standard of force. We observe that this is the standard approach for instrumented indentation equipment, with sensors typically calibrated in situ by the hanging of small masses from the load head. Such a procedure has even been attempted for atomic force microscopy (AFM)[14] where microsphere weights were attached to the end of the cantilever sensor. This is by far the most direct application of existing force realization practice, however, it is plagued by the aforementioned uncertainties of mass, not to mention that the procedure seems prohibitively difficult to execute for the atomic force microscope.

In the second approach, the example machine is calibrated using a transfer artifact or secondary force standard. This secondary force standard is, in fact, another load cell that has been calibrated against a primary standard of force. Once again, the unit of force is disseminated from a primary standard to the testing machine, this time through calibration of an intermediary load cell. The accuracy of this second approach, at least for macroscale devices, is inferior to the first due to the added complexity of interfacing the two load cells, but it is more convenient. At the microscale, calibration procedures built around a secondary standard appear to produce better precision. Some success has been reported in the force calibration of atomic force microscope systems through the use of so-called calibration cantilevers.[15–17] The procedure consists of pressing a cantilever of unknown stiffness against a calibration cantilever of supposedly known stiffness. The stiffness of the calibration cantilever is known to the extent that it is computed from estimates of its cross-section dimensions and modulus of elasticity.[16] The stiffness of cantilever load cells has also been determined by probing them against a mass balance using an appropriately calibrated scanning stage.[17] This latter experiment uses a mass balance as a comparator between deadweight and elastic forces in a fashion similar to the work considered here.

The test forces available by treating a mass balance as a transfer standard are well suited to instrumented indentation of metals (the so-called nanorange between 1 μN and 2000 μN specified in ISO14577), although the form factor of a mass balance is often inconvenient (e.g., too large to fit on a specimen stage). Nevertheless, traceable forces can be derived from mass and gravity and transferred to a load cell of more suitable form factor using the balance as an intermediary, provided loading axes are aligned properly with gravity. In fact, it is only a desire to extend traceability to the much smaller forces typical of atomic force microscopes, which drives the development of the electrostatic force generator described in the

Downloaded from http:/www.cambridge.org/core. the NIST Virtual Library (NVL), on 27 Sep 2016 at 19:16:31, subject to the Cambridge Core terms of use, available at http:/www.cambridge.org/core/terms.
http://dx.doi.org/10.1557/jmr.2004.19.1.366

previous section. The goal is traceable nanonewtons, and this cannot be achieved via conventional balances. An instrumented indenter possessing its own electrical force generator and having a resolution of nanonewtons might provide a good start. However, such devices are not designed explicitly to produce a force that can be computed from first principles application of the appropriate electromagnetic theory. In their current form, they must be calibrated ultimately through comparison to dead weight. And, as has been observed, 5 μN is the smallest available deadweight-generated force. Relying on the instrument to generate test forces below this level would be trusting to the linearity of the indenter's force generator, which is likely to be very good, but hard to trust once levels fall below 0.5 μN.

In summary, what we seek in a microscale load cell, through analogy to conventional large-scale force practices, is a device with a well defined loading point, responsive to loads only along a well-defined axis, and possessing its own sensor for converting the load to a usable readout. This readout is preferably a voltage that is repeatable to a few tenths of an mV/V. This load cell should be capable of use in either of the two calibration approaches. To be compatible with atomic force microscope–style probe force instruments, the load cell should be of a size compatible with both the sensor and specimen holders common in commercial atomic force microscope devices. Similarly, sensors compatible with the working space of commercial instrumented indentation equipment are also desirable, though this geometry is less restrictive.

A. Atomic force microscope force sensors

Within the context of commercial atomic force microscope equipment, there is a fairly limited selection of sensors in the desired micro- to nanonewton force range, with the vast majority based on a cantilever elastic load element that deflects in response to the applied load. Such cantilever sensors usually have a sharp tip that provides the requisite well-defined loading point; however, from a metrology standpoint, this arrangement fails to define a single measurement axis because a cantilever will also respond to moments occurring at the point of contact. Ideally, a constrained load element, such as a parallelogram flexure, is preferable, though few examples of such devices exist on this scale, and no commercial examples could be found.

The detection schemes used to measure the elastic deformation of scanning-probe cantilevers, such as capacitive, interferometric, and the well-known optical lever arm techniques,[18] present another set of problems for accurate force metrology. For instance, all of these techniques measure the deformation by recording the displacement at a given point on the cantilever. Typically, they use an externally supplied reference frame to monitor this deflection and produce the force readout. Clearly, the displacement calibration of these instruments can vary greatly with set-up and alignment of the cantilever with respect to the external frame of reference. Direct calibration of such devices against the EFB is conceivable, but awkward, because it requires positioning the entire atomic force microscope over the EFB. It also seems we cannot easily use these devices as secondary force standards because the force calibration is preserved only as long as the cantilever remains aligned with the atomic force microscope's displacement measuring metrology frame. Previous calibration approaches have focused on determining the spring constant of the load element[14–20] because in principal this can be determined independent of the detection hardware and results in an artifact with a calibration that can be transferred from instrument to instrument. However, embracing this approach requires that the detection scheme eventually be calibrated as an absolute displacement, otherwise the calibration remains setup dependent.

There are cantilever sensors that measure strain rather than displacement. This approach has the advantage of keeping the metrology local to the cantilever. The strain measurement is achieved using the well-known piezoresistance phenomenon. Piezoresistance occurs in metals and semiconductors and refers to a variation of bulk resistivity of a material with applied stress. This effect can be used to sense strain in elastic load members as a change in resistance and is sometimes referred to as a solid-state strain gauge. It has been used in various pressure detection schemes since its discovery and has successfully been applied to the atomic force microscope to achieve atomic resolution imagery.[21] As applied in atomic force microscopes, a resistor is typically doped into a region of material at the base of a silicon cantilever. The nominal resistance is a function of dopant concentration (typically boron) and can be fabricated using known relationships about semiconductor properties. Deflection of the cantilever by an applied force causes the resistance of the cantilever to vary about its nominal value, the sign and magnitude of deviation depending on the net change in stress experienced in the doped region. The resistance can be observed using a Wheatstone bridge or Ohm meter of sufficient resolution. Hence, this method of load detection has much in common with traditional strain-gauge-based load cells used as secondary force standards, albeit at a much smaller scale.

Cantilevers composed of piezoresistive material as described above are available commercially, and a photo of the type of cantilever purchased for use in our experiments is shown in the inset of Fig. 3, accompanying a plot of the typical "open circuit" terminal voltage of the device. The force sensitivity is nominally 500 nN/Ω,

Downloaded from http:/www.cambridge.org/core. the NIST Virtual Library (NVL), on 27 Sep 2016 at 19:16:31, subject to the Cambridge Core terms of use, available at http:/www.cambridge.org/core/terms. http://dx.doi.org/10.1557/jmr.2004.19.1.366

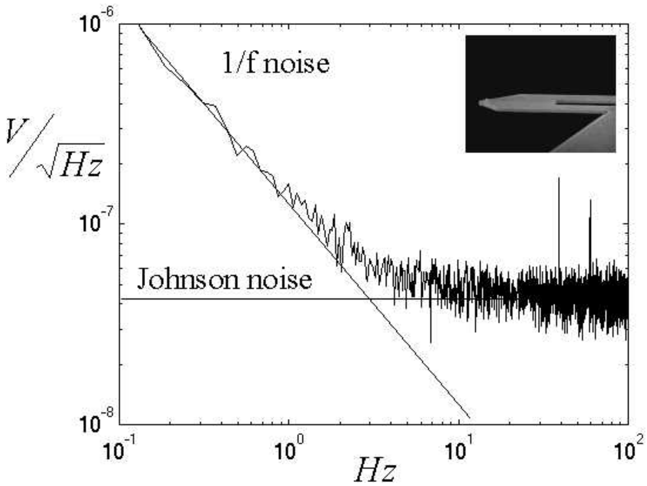

FIG. 3. Open circuit terminal voltage as a function of frequency showing regions of different noise phenomena.

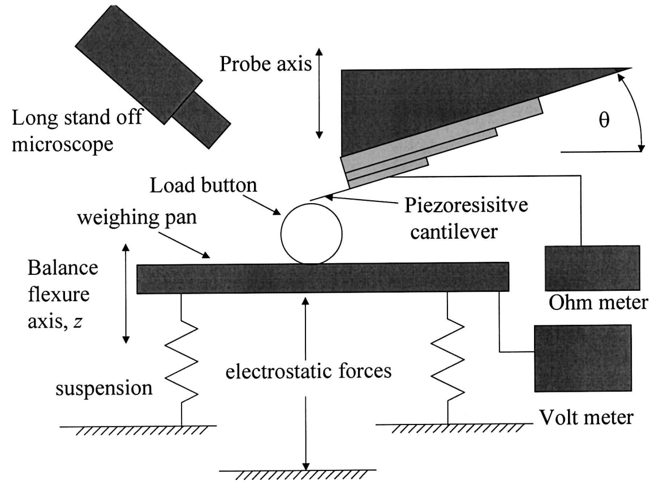

FIG. 4. Schematic of cantilever calibration set-up. Load button is a polished ruby spherical lens, 3 mm in diameter.

with a low frequency force noise of 0.4 nN when integrated between 10 Hz and 1000 Hz, according to the manufacturer's specification. In our experience with "direct current" force measurements using these sensors, we seldom achieved better than 10 nN in resolution because the noise performance below 10 Hz becomes dominated by 1/f noise in the detection electronics or piezoresistor itself. The plot of open-circuit voltage as a function of frequency shown in Fig. 3 reveals this trend. In this plot, we distinguish between regimes where the noise has a predominately 1/f character and where the noise has a flat spectrum typical of Johnson noise.

Thus far, the low-frequency noise has limited the application of these devices in force microscopy, with the vast majority of systems still choosing optical detection. However, there is recent evidence that careful design can manage these noise problems and produce sensors with resolutions that meet or exceed that achieved using optical detection schemes, with demonstrated low-frequency resolution at or below 3 pN.[22] Finally, we observe that both the nominal resistance and stress sensitivity of a piezoresistor may vary with temperature.[23] This temperature dependence must be considered and preferably quantified if such devices are to be developed as force artifacts, and this issue remains to be studied.

IV. CALIBRATION OF A PIEZORESISTIVE CANTILEVER

A. Setup

The EFB was probed using the previously discussed commercial piezoresistive cantilever, as illustrated schematically in Fig. 4. In this experiment, the cantilever had a nominal resistance of 3.04 kΩ, length of approximately 3×10^{-4} m, thickness of approximately 3 μm, total width of 50 μm, and a published spring constant of 1 N/m (all according to the manufacturer's specification). Changes in resistance were recorded using a metrology-grade resistance meter with a two-wire connection. The cantilever chip came mounted on a ceramic base with gold contacts, to which we soldered two wire leads made from 0.25-mm-diameter magnet wire.

An obvious issue to be addressed in the development of a standard load cell for atomic force microscopes will be a methodology for fixing the orientation of the device with respect to the EFB load button. We chose to use the ceramic base of the piezoresistive sensor as a reference surface, gluing the cantilever assembly to a glass microscope slide, which was then clamped in a fixture, making an angle of approximately 14° between the plane of the cantilever and a plane normal to the balance axis. The angle was selected as representative of the nominal angle used in typical AFM instruments, though, to our knowledge, no standard orientation exists. The fixture was attached to a combination coarse and fine adjustment three-axis scanning stage for probing the balance. In these initial experiments, no attempt was made to align the probe axis to the balance flexure axis (i.e., with gravity), though this too will be important in developing a standard procedure.

B. Procedure

The cantilever was brought into contact with the top of the balance load button by manually turning a micrometer screw on the z axis of the three-axis stage. A ruby sphere 3 mm in diameter with 0.64-μm sphericity served as the balance load button. This sphere is a precision optical component possessing a polished surface, and it appeared "smooth" within the resolution of a long stand-off microscope (of the order a few micrometers) used during the experiment to observe the physical point of contact. Upon contact, the force was sensed as a change

Downloaded from http:/www.cambridge.org/core. the NIST Virtual Library (NVL), on 27 Sep 2016 at 19:16:31, subject to the Cambridge Core terms of use, available at http:/www.cambridge.org/core/terms. http://dx.doi.org/10.1557/jmr.2004.19.1.366

in resistance, and an arbitrary small preload was applied corresponding to a few ohms.

An automated fine motion scan was next executed using an electrostrictive actuator to drive the *z* stage, pushing the cantilever into the balance load button. The stage was displaced a fixed increment, the balance allowed to settle back to null, and then the balance servo voltage recorded while the resistance value was read from the Ohm meter. The stage was scanned in and out through six such increments, each nominally 5 μN, producing a maximum load of approximately 30 μN. Although the sensor is well suited to measure forces between 0.1 μN and 10 μN, a 5-μN load increment was the smallest that could be resolved with the desired accuracy. A smaller increment will improve confidence in the low force sensitivity, but will have to wait for the next-generation balance.

The load and unload sequence was repeated between 20 and 100 times using a fully automated scheme to yield a complete set of measurements over a period of between 1 and 5 h (nominally 3 min per scan). From time to time, the calibration of the EFB was verified by measuring the capacitance gradient. A comparison of the EFB to deadweight force was also performed using nominal 10 μN and 100 μN loads. These crosschecks verified balance performance to a few nN/μN, sufficient accuracy for these experiments.

C. Results

The resistance and voltage data acquired by the automated system for each scan were fitted with a polynomial equation of the following form using the method of least squares

$$F_i = \tfrac{1}{2}\frac{\mathrm{d}C}{\mathrm{d}z}\left(U_i^2 - \frac{\sum_1^n U_i^2}{n}\right) = p_0 + p_1\delta R_i + p_2\delta R_i^2 \ldots p_n\delta R_i^n \quad , \tag{3}$$

where F_i = contact force component along flexure axis at load increment *i*, N; d*C*/d*z* = capacitance gradient along flexure axis, pF/mm; U_i = EFB potential at load increment *i*, V; δR_ι = deviation in resistance from the mean, Ω; and p_n = polynomial coefficients.

A first-degree polynomial was sufficient for this data, based on the observed structure of the residuals. Thus, it was possible to determine the slope and hence the sensitivity for a given scan. The data for each scan were normalized about the mean load and resistance values in an attempt to account for drift in both the balance and sensor. The estimated sensitivity for the cantilever is reported as the average of these fits, with the standard deviation of the slopes indicating the repeatability of the set-up (error bars in Fig. 5). The cantilever was then retracted from the balance along the vertical axis and parked off to the side. This entire experiment was repeated on a variety of dates. The results are summarized in Fig. 5.

D. Uncertainty

The EFB measures the component of force along the balance axis. This force is calculated as

$$F_i = \tfrac{1}{2}\frac{\mathrm{d}C}{\mathrm{d}z}\left(U_i^2 - \frac{\sum_1^n U_i^2}{n}\right) \quad , \tag{4}$$

where the capacitance gradient d*C*/d*z* is measured along the axis defined by the guiding flexure that supports the suspended inner electrode of the EFB. Using a careful alignment procedure,[11] we have ascertained that this axis, gravity, a translation stage for moving the inner electrode support, and the interferometer measurement axis are all aligned within 3 mrad. In the current experiment, the gradient was periodically measured along this direction and assigned a value of (0.9430 ± 0.0005) pF/mm. Greater accuracy can be achieved,[11] but was not warranted. We note that the gradient has been observed to change in a systematic fashion at the level of 0.001 pF/mm depending on the type and orientation of staging used around the load button. This illustrates the need for better electrostatic and magnetic shielding of the electrodes so that stray charges and fields do not affect the EFB sensitivity. The absolute orientation of the probe axis with respect to the balance axis was not determined. We estimate the axis was aligned with respect to gravity within only 5°, but that this uncertain alignment was repeatable at a level less than 5 mrad. Thus, while cosine errors as large as 0.4% are possible if the transducer is used in another instrument, for the purposes of testing the repeatability of our own instrument, variations in alignment from test to test appear negligible.

The uncertainty in *U* arises from the uncertainties in the measured gain and offset errors of the voltmeter and the measured ac noise on the high-voltage supply. These errors are small and when combined contribute less than a part in 10^5 to the uncertainty of a force determination.

Finally, the noise floor of the balance was observed to be 25 nN in these experiments, which is almost twice the value that was observed in previous deadweight comparisons.[11,12] We suspect the additional noise may be attributed to the removal of one side of a large shielding box that surrounds the experiment to accommodate the long stand-off microscope.

E. Limitations

The EFB measures only one component of the contact force, and error terms can arise due to the friction force

Downloaded from http:/www.cambridge.org/core. the NIST Virtual Library (NVL), on 27 Sep 2016 at 19:16:31, subject to the Cambridge Core terms of use, available at http:/www.cambridge.org/core/terms. http://dx.doi.org/10.1557/jmr.2004.19.1.366

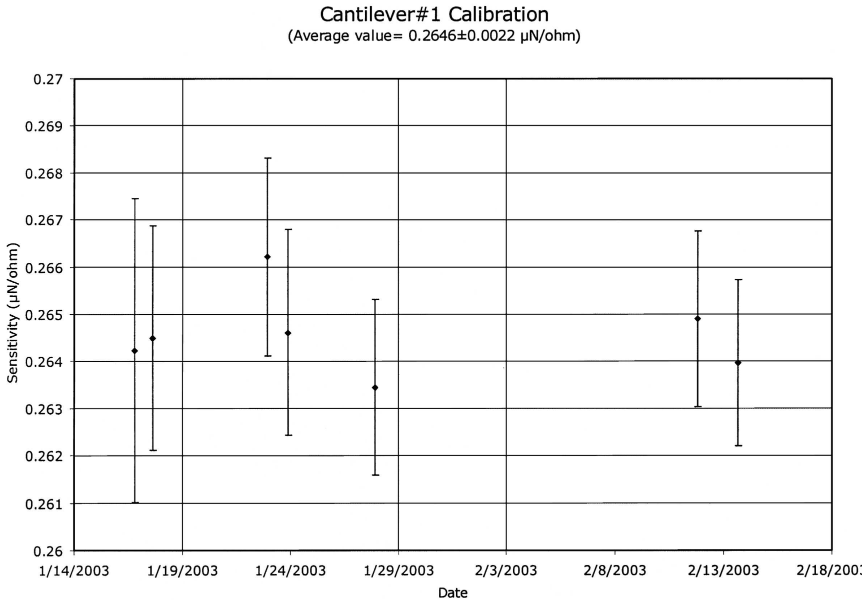

FIG. 5. Mean sensitivities determined for standard no. 1 on seven different occasions. Error bars correspond to 1 standard deviation.

that occurs between the probe tip and balance load button. Though we did not make quantitative measurements of this interaction, it seems worthwhile to ponder at least a simple model of the mechanics of the problem in hopes that it may illuminate the potential influence of friction on the uncertainty of the measurement.

Consider the freebody diagram of Fig. 6, where the piezoresistive cantilever is illustrated as a rotary hinge of length l pivoting about the sensor at the origin o. The normal and tangential forces acting at the tip result in bending stresses

$$\sigma_{b,o} \approx \frac{3}{bt^2}[F_n(l \cos \phi) - F_t(l \sin \phi)] \quad , \tag{5}$$

and axial stresses

$$\sigma_{a,o} \approx \frac{F_n \sin \phi + F_t \cos \phi}{2bt} \quad , \tag{6}$$

at the origin, where $\sigma_{b,o}$ is the total bending stress at the surface of the beam at the origin, $\sigma_{a,o}$ is the total axial component of stress, $t = 3$ μm is the beam thickness, $b = 18$ μm is the width of the beam legs, $h = 4.5$ μm is the height of the tip, $l = 245$ μm is the effective lever arm, F_n is the component of the contact force acting normal to the load button surface and F_t the component tangent to this surface, and ϕ is the contact angle, which varied between approximately 8° at fully loaded to 14° at loss of contact. It is important to keep in mind that the cantilever is not rigid, and that the off-axis forces can make significant the local deviation from the standard beam bending theory that is assumed here. The degree to which axial stress is a factor depends on the slenderness ratio l/t. For typical cantilevers, the axial component accounts for less than 0.5% of the stress.

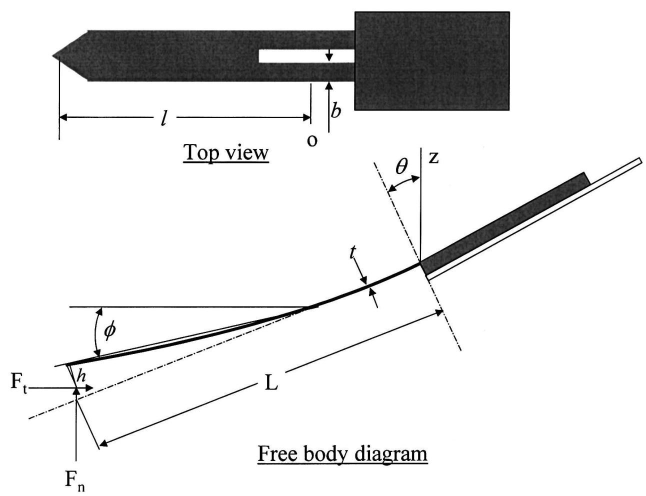

FIG. 6. Planview and freebody diagram of piezoresistive cantilever under loading.

Stresses due to the normal component of force represent desired signal, whereas stresses produced by the tangential or friction component are unwanted and contribute an error because their contribution to the change in piezoresistance cannot be distinguished from that caused by the normal force. Taking the ratio between bending stresses due to friction and those due to the normal contact force, the percentage error due to friction forces may be approximated for small angles as

$$\% \text{ error} \approx \pm \mu\phi \times 100\% \quad , \tag{7}$$

Downloaded from http:/www.cambridge.org/core. the NIST Virtual Library (NVL), on 27 Sep 2016 at 19:16:31, subject to the Cambridge Core terms of use, available at http:/www.cambridge.org/core/terms. http://dx.doi.org/10.1557/jmr.2004.19.1.366

where the sign is determined by the direction of the friction force, μ is the coefficient of friction, and we have assumed $F_t = \mu F_n$.

Suppose the tip sticks to the surface of the ruby sphere during a calibration. For this case, the maximum friction force possible between the two surfaces can be found using the coefficient of static friction. Letting $\phi = 10°$ and assuming a static coefficient of friction of 0.6, we obtain a value of –10% as a crude, upper bound on the error contribution of the friction force.

Suppose now that the tip slides along the surface of the ruby sphere. In this case, the tangential force must exceed the force due to static friction for sliding to occur. However, once sliding, the friction force is of a magnitude determined by the kinetic coefficient of friction. We assume that when the cantilever comes to rest, and a load increment is recorded, the tangential component of force is at most as large as that due to kinetic friction. Assuming a kinetic coefficient of friction of 0.3 and using the previous value of the contact angle, we obtain a bounding value of –5% for the error contribution of this type of friction force. The sign on the error is due to the assumption that the tip slides away from the origin as the cantilever is pressed into the balance. For a slipping condition, we expect the sign to reverse on retraction. Evidence of this behavior should appear as hysteresis at the transition from loading to unloading.

There are a number of approaches available to deal with this problem. The most straightforward and most restrictive is to insist that the calibration is only valid for applications that precisely mirror the geometry and contact conditions used during calibration. Another, less restrictive approach is to make the contact angle as small as possible to minimize the tendency to build up tangential force. This can effectively be achieved by making the scan axis normal to the cantilever, rather than the balance. Another possible avenue is to develop compensation schemes. For instance, the sensitivity to axial load could be eliminated using a second sensing element on the opposite side of the beam. A differential measurement would enhance sensitivity to bending while effectively eliminating sensitivity to axial loading. Software compensation based on physical modeling could also be used, provided the physics of the contact condition were better understood.

F. Discussion

The response of the piezoresistive cantilever was linear over the range of force used in the calibration (approximately 30 μN). The standard deviation of residual forces after fitting with a first-order calibration equation was approximately 170 nN. The observed noise floor of the balance during deadweight experiments was 25 nN. The piezoresistive sensor appeared stable to approximately 0.05 Ω within the time frame of a single measurement, suggesting a noise equivalent of force of approximately 12 nN. This implies that the standard deviation of the calibration procedure is within an order of magnitude of the resolution of the devices, so we are not yet noise limited.

The relative standard deviation of the computed sensitivities for each of the seven experiments shown in Fig. 5 was consistently below the 1% level, averaging approximately 0.8% of the mean value of 264.6 nN/Ω. Scatter of the means from day to day was even lower at 0.3%, suggesting that the procedure is reproducible. The sensitivity is thus $s_1 = (264.6 \pm 0.8)$ nN/Ω, where the uncertainty is simply the standard deviation of the mean of the seven measurements, with all other contributions being negligible. This uncertainty is limited to the geometry used in our laboratory. Adding to this the estimated alignment uncertainty yields $s_1 = (264.6 \pm 2)$ nN/Ω.

Hysteresis due to the previously described friction effects was not detected at the transition from loading to unloading, suggesting either that the tip stuck to the ruby sphere or perhaps more likely that the friction was very low for this contact. The uncertainty associated with this behavior will have an impact if, as is the intent, the cantilever is used as an artifact standard in other geometries contacting other materials. Further study is required, but based on the previous simple mechanics based arguments, the standard could produce an error as high as 10% of the load for conditions that result in sticking at the interface.

Other factors that were not measured, such as surface roughness of the load button, shape of the cantilever tip, temperature dependence of piezoresistance, and so forth, may effect the ability of others to reproduce these results outside of our laboratory and will be the subject of subsequent investigations.

V. ATOMIC FORCE MICROSCOPE CALIBRATION USING A PIEZORESISTIVE CANTILEVER

The force sensitivity of a piezoresistive cantilever was calibrated in the fashion described in the previous section, and then the sensor was secured on the specimen stage of a commercially available atomic force microscope–style force measurement device. We will refer to this calibrated sensor as force standard no. 2 in the subsequent discussions. Sensor no. 1 described in the previous section broke through mishandling, yet another challenge in the development of these calibration procedures.

The experiment consisted of probing force standard no. 2 with a conventional atomic force microscope probe. The atomic force microscope in this instance was of the type designed explicitly for obtaining force curves and

Downloaded from http:/www.cambridge.org/core. the NIST Virtual Library (NVL), on 27 Sep 2016 at 19:16:31, subject to the Cambridge Core terms of use, available at http:/www.cambridge.org/core/terms. http://dx.doi.org/10.1557/jmr.2004.19.1.366

uses an optical lever arm to detect motion of a cantilever load element with respect to a precision vertical scanning stage. The atomic force microscope includes an inverted microscope for viewing the orientation of its probe cantilever with respect to the fixed specimen stage. This optical view of the experimental workspace was supplemented using a small (300 μm on a side) turning mirror to allow a "side" view of the cantilever and force standard simply by refocusing the optic. This proved useful during the alignment of the cantilever tip with respect to the force standard. A schematic of the set-up is shown in Fig. 7.

A. Procedure

A conventional V-shaped, micromachined silicon cantilever was mounted in the atomic force microscope according to the procedures outlined by the atomic force microscope manufacturer. The tip selected for these experiments was fairly rigid, having a length of 85 μm, leg width of 18 μm, tip height of approximately 6 μm, tip radius of curvature of around 10 nm, and a stiffness of 13 N/m, all according to the manufacturer's published specification. The tip of this cantilever was brought into contact with force standard no. 2 by using the manual adjustment screws on the atomic force microscope head and the x, y positioning screws on the specimen stage. The contact point was as near the tip of the force standard as possible, though it was necessary to offset the point of contact because it was not possible to touch tip to tip during a calibration and obtain clean data.

Once suitable contact was made, the atomic force microscope was set into continuous scan mode. In this mode, the precision z-stage of the atomic force microscope cycled continuously through a range of motion that caused full-scale output of the optical lever (approximately 5 μm). An automated system then recorded the

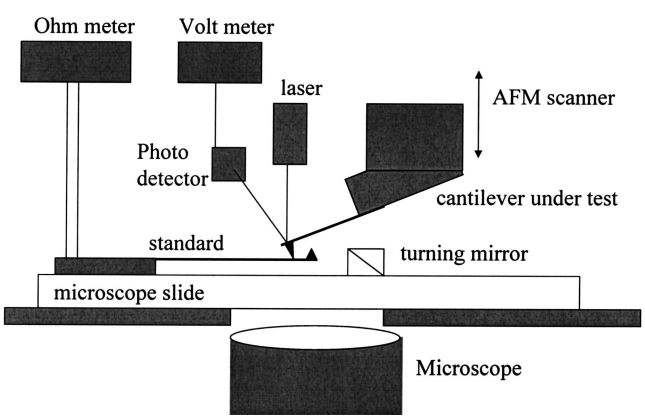

FIG. 7. Arrangement of the experimental components used for atomic force microscope calibration. The standard was mounted on a microscope slide and the experiment viewed through an AFM inverted microscope. A side view of the cantilever contact could be seen using a small turning mirror located near the standard.

output of the atomic force microscope's optical lever as a function of the measured force. This was accomplished using a data acquisition computer to sample simultaneously the voltage output of the photodetector and the change in resistance measured across the piezoresistor. Both values were measured using metrology-grade multimeters with internal standards traceable to NIST.

The atomic force microscope stage was allowed to scan through its full range of travel at least 10 times during a calibration experiment. After this, contact was broken, and the standard was removed and examined under an optical microscope to inspect for damage. The standard was then returned to the atomic force microscope specimen stage, the cantilever and standard realigned, contact made, and the scanning repeated.

B. Results

The sensitivity of force standard no. 2 was measured using the EFB and the previously described procedures. The sensitivity was found to be (807 ± 8) nN/Ω. Data on the long-term repeatability of this number are not yet available, but it is presumed it will be similar to that achieved for standard no. 1.

Data taken while performing force scans with the atomic force microscope were processed in a fashion similar to that used during the calibration of the force standard. Atomic force microscope force scans were continuous, however, in contrast to the stepwise scans used during the standard calibration. Hence, data were taken at regular intervals in time, not necessarily at regular intervals of load.

Contact forces were computed using the measured sensitivity of standard no. 2 multiplied by the change in resistance from the nominal, unloaded value at the start of each scan. Contact forces as a function of photodetector output, V_p, were curve fit with a least squares polynomial calibration equation of the following form:

$$F_i = s_2 \delta R_i = c_0 + c_1 \delta V_{p,i} + c_2 \delta V_{p,i}{}^2 \ldots c_n \delta V_{p,i}{}^n \quad , \tag{8}$$

where F_i = contact force at increment i, N; s_2 = 807 nN/Ω, sensitivity of standard no. 2; $\delta R_\iota = R_i - R_0$, change in piezoresistance from initial value, Ω; $\delta V_{p,I} = V_{p,i} - V_{p,0}$, change in photodetector output from initial value, V; and c_n = polynomial coefficients.

Figure 8 shows the results of a linear fit of the data along with a plot of the differences, or residuals, between the individual values observed in the calibration and the corresponding values taken from the first-order fit. The residuals shown in Fig. 8 show evidence of higher-order structure and hysteresis, with a standard deviation of 190 nN. Future investigations will examine the origins of this hysteresis and its potential connection to the previously discussed friction at the contact interface.

Downloaded from http:/www.cambridge.org/core. the NIST Virtual Library (NVL), on 27 Sep 2016 at 19:16:31, subject to the Cambridge Core terms of use, available at http:/www.cambridge.org/core/terms. http://dx.doi.org/10.1557/jmr.2004.19.1.366

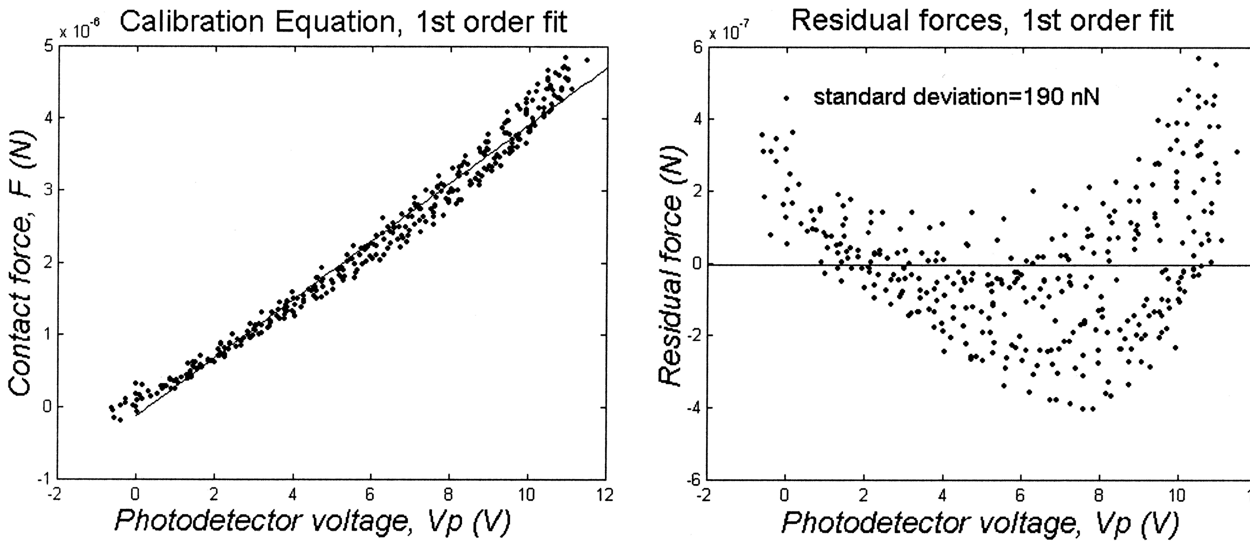

FIG. 8. Results obtained by a first-order polynomial curve fit of the entire data set.

To account for the higher order structure of the residuals, the data points were reanalyzed using a second-order calibration equation, this time fitting only the ascending force values. These results are shown in Fig. 9. Residuals are smaller and far more random for the second-order fit than was the case for the linear curve fit. The standard deviation of the residual forces is now 83 nN, or approximately 2% of the full-scale load.

The experiment was repeated to begin assessing the repeatability of the procedure because accuracy in the alignment of the cantilever tip and standard is suspect. As a metric for comparison, approximate atomic force microscope sensitivity was computed by evaluating the derivative of the calibration equation at a photodetector voltage of 5 V, near the midpoint of the force scan. Each ascending force scan was fit and a value of sensitivity determined in this fashion. The mean sensitivity and its standard deviation obtained from the data of the first experiment was (417 ± 12) nN/V whereas from the second experiment, we obtained (439 ± 11) nN/V. Taking the mean of the two experiments, we obtain a sensitivity of s_{AFM} = (428 ± 12) nN/V as an uncorrected estimate of the force sensitivity of the atomic force microscope at a nominal compressive load of 2.14 μN.

C. Corrections

Tip-to-tip contact between the cantilever and standard was not possible during a scan. The actual contact condition is illustrated in the photos of Fig. 10, along with a schematic of the interaction. Note the photos are taken using the available infrared illumination from the laser so that the silicon is somewhat translucent.

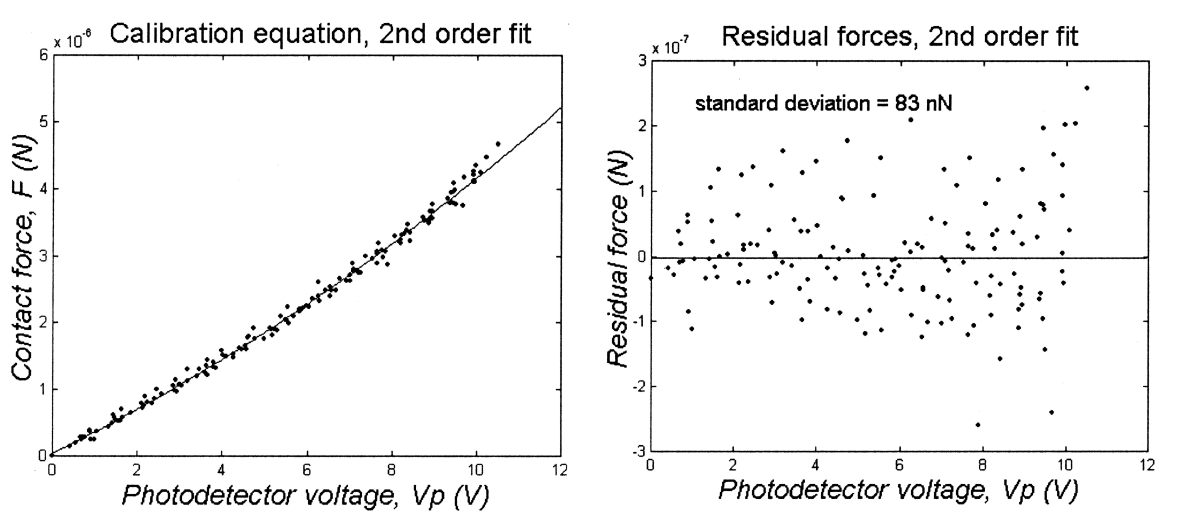

FIG. 9. Results obtained from a second-order polynomial curve fit of only the ascending force data.

Downloaded from http:/www.cambridge.org/core. the NIST Virtual Library (NVL), on 27 Sep 2016 at 19:16:31, subject to the Cambridge Core terms of use, available at http:/www.cambridge.org/core/terms. http://dx.doi.org/10.1557/jmr.2004.19.1.366

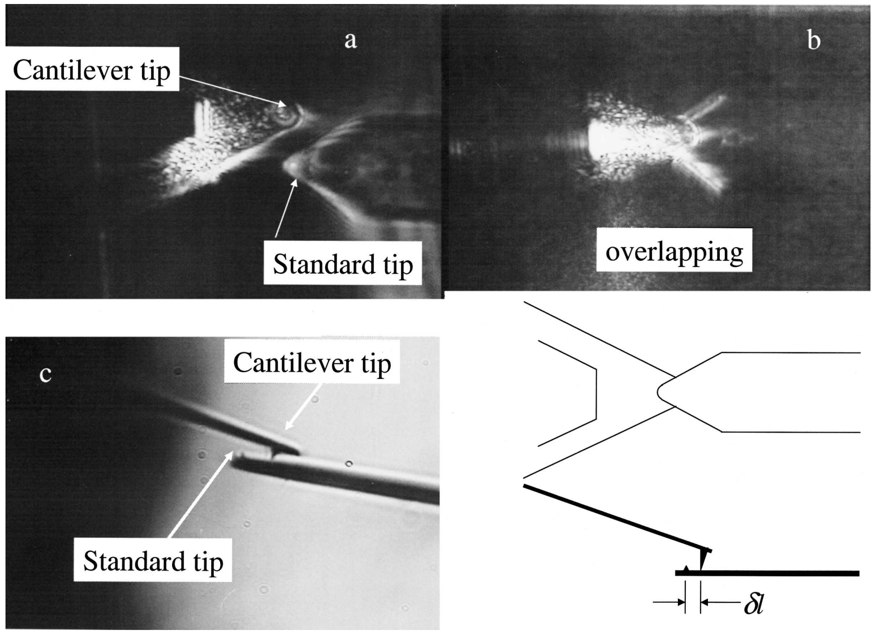

FIG. 10. Views of the cantilever and standard during calibration: (a) bottom view, tips misaligned laterally; (b) bottom view, tips overlapping; and (c) side view through turning mirror of tips with longitudinal misalignment

We believe contact was within ±5 μm of the centerline of the standard and assume that variations due to uncertainty in lateral displacement with respect to the centerline are negligibly small. In principal, the resulting torque produces tensile stresses on one side of the centerline that are balanced by compressive stresses on the other, so the net change in piezoresistance is zero. Deviations from symmetry are expected, however, and this result remains to be quantified.

The effect of longitudinal misalignment is clear because it has direct impact on the moment produced with respect to the base of the standard. Assuming only that the change in the piezoresistance is proportional to stress and that the stress is proportional to the moment produced by the application of a point force along a beam of effective length l, we estimate that the contact force should be corrected as follows:

$$F = s_2 \delta\Omega \cdot \frac{l \cos\theta - h \sin\theta}{l - \delta l} \quad , \tag{9}$$

where l = effective lever arm of force standard, δl = offset of contact point from tip of standard, h = tip height of cantilever force standard, and θ = nominal contact angle during calibration of s_2.

This corrects for the load offset and the fact that the standard was oriented at an angle θ with respect to a direction normal to the force during calibration of s_2. A tacit assumption has been that the force at contact is normal to the neutral axis of the standard and that the orientation of this axis changes negligibly under load. Furthermore, the longitudinal location of the contact point is assumed not to change as a function of the loading, (i.e., the cantilever tip does not slide appreciably along the surface of the standard). These assumptions seem reasonable given the fairly small angular displacements experienced by both the standard (≈0.02 rad based on a maximum deflection of 5 μm) and the cantilever (≈0.006 rad based on a maximum deflection of 0.5 μm) during this experiment. Finally, we reiterate that this analysis considers only the effect of the normal force and makes no corrections for possible contributions from frictional forces. In general, off-axis moments about the atomic force microscope tip might cause local rotation/buckling. We are unable to account completely for these effects using only our simple model. However, the atomic force microscope cantilever is significantly stiffer (approximately an order of magnitude) than the standard cantilever, and it seems likely that rotation- and buckling-induced errors that would affect its optical beam bounce detection scheme are negligible. Furthermore, the standard experiences a maximum variation of contact angle of only 0.02 rad, leading to a possible friction-induced load error in the standard of approximately 1% of the contact force, assuming the previous coefficient of friction. The entire problem could perhaps be minimized if the atomic force microscope scan axis were to use a lateral compensation angle, as discussed in Ref. 24.

An attempt was made to measure the offset δl for each experiment. The procedure consisted of photographing a transparent objective micrometer scale with 10-μm pitch

Downloaded from http:/www.cambridge.org/core. the NIST Virtual Library (NVL), on 27 Sep 2016 at 19:16:31, subject to the Cambridge Core terms of use, available at http:/www.cambridge.org/core/terms. http://dx.doi.org/10.1557/jmr.2004.19.1.366

using the high-magnification inverted microscope. This image was then superimposed on images of the cantilever and standard to provide a ruler for measuring the degree of longitudinal misalignment. Example images from an experiment are shown in Fig. 11. Using this technique, it was possible to establish the deviation of tip alignments to within approximately 1 μm. In the first experiment, we estimate $\delta l = 12$ μm whereas in the second experiment, $\delta l = 11$ μm.

Applying the above correction using $l = 245$ μm, $h = 4.5$ μm, $\theta = 0.244$ rad, and the appropriate value of δl, we compute corrected estimates of the atomic force microscope sensitivity and find $s_{\mathrm{AFM}} = (420 \pm 12)$ nN/V in experiment one, and $s_{\mathrm{AFM}} = (442 \pm 11)$ nN/V in experiment two. Although these two experiments agree within experimental uncertainty, a discrepancy on the order of 5% may be present. The result was deemed adequate for the proof-of-concept. A future focus of this work will be to investigate the issues associated with reproducing these results and examining the potential systematic errors, particularly regarding the influence of the contact condition.

We conclude that the misalignment is small and could effectively be eliminated simply by using a tipless standard, or the back side of this sensor. Likewise, the EFB could be equipped with a load button more like an indenter tip. The standard could then be calibrated against a point contact in a fashion consistent with its subsequent use as a secondary force standard. The force sensitivity dependence on alignment could be mapped, rather than relying on a model-based correction.

D. Discussion

It is worth contrasting the above results with those obtainable using typical practices. For instance, it is common to use the manufacturer's published cantilever stiffness value along with a calibration of the optical lever displacement sensitivity to arrive at a value for force. The optical lever arm sensitivity is typically determined by probing a hard specimen, with the displacement of the cantilever tip inferred from the measured displacement of the cantilever base. The commercial platform used in this experiment includes a calibrated linear variable displacement transformer (LVDT) that records the displacement of the atomic force microscope scan axis. It also provides software for fitting the relationship between displacement and photodetector output with a straight line to estimate the optical lever displacement sensitivity (OLS).

TABLE I. Optical lever sensitivities.

Displacement range (nm)	Optical lever sensitivity (nm/V)
0–100	42.0
100–200	44.6
200–300	49.2
300–400	53.8
400–500	60.0

Measured values of the OLS appear in Table I. The results suggest that the OLS is nonlinear, explaining the need for the higher-order curve fit in the calibration of Fig. 8. Working from the table, a force sensitivity can be estimated using the appropriate optical lever sensitivity and the manufacturer's estimate of the cantilever stiffness, or $s_{\mathrm{AFM}} = \mathrm{OLS} \times k$. For a nominal photodetector output $V\mathrm{p} = 5$ V, the displacement is between 200 and 300 nm, so that OLS $= (49.2 \pm 5)$ nm/V. Our assignment of an uncertainty to the OLS is based solely on the linearization and assumes that the uncertainty of the LVDT calibration is negligible and that the frame compliance and contact compliance are small in comparison to the cantilever compliance. The published cantilever stiffness is $k = 13$ N/m with no stated uncertainty. We note that it has been asserted elsewhere[25] that even the most accurate published values have uncertainties of ±50%. Thus, the force sensitivity based on the published spring constant and measured OLS is $s_{\mathrm{AFM}} = (640 \pm 320)$ nN/V. In contrast, the estimated value based on direct comparison to the secondary force standard is (431 ± 12) nN/V. In the future, we will explore the instrumented indentation method of Ref. 19 to obtain a better estimate of the cantilever stiffness and produce a better crosscheck on our procedures.

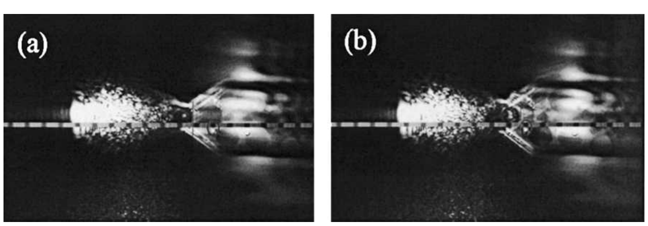

FIG. 11. Measuring the tip offset distance using an objective micrometer with 10-μm ticks. In photo (a), tips are touching as determined by listening to the optical lever signal. A small feature is found on the standard as a reference point, and the distance between the cantilever nose and the feature is recorded. In photo (b), the tips have been offset by approximately 9 μm with reference to (a).

VI. CONCLUSIONS

We have presented a proof-of-concept method for calibrating a scanning probe force sensor as a load cell in a manner traceable to the SI using standards maintained at NIST. This "load cell" was subsequently used to establish the force sensitivity of an AFM-type laboratory instrument, fulfilling the role of a secondary force standard. The force magnitudes in these experiments are new to the world of SI force calibration, as is the manner in which they were ultimately realized through electrostatic rather than gravitational phenomena.

Downloaded from http:/www.cambridge.org/core. the NIST Virtual Library (NVL), on 27 Sep 2016 at 19:16:31, subject to the Cambridge Core terms of use, available at http:/www.cambridge.org/core/terms. http://dx.doi.org/10.1557/jmr.2004.19.1.366

A host of transduction schemes are available for contriving small force sensors, and, based on criteria for a self-contained device, we elected to examine a piezoresistive cantilever. Results with this commercial force sensor were both repeatable and reproducible below the level of a percent for a given contact condition and maximum loads of several micronewtons. Limitations on the transfer accuracy of this device were identified owing to cross-axis sensitivity of the sensors to friction. We attempted to place an upper bound on this effect by using a very simplified analysis. For the simple case modeled, we determined that the systematic error could be as high as 10% of the nominal load considering typical coefficients of static friction. Such an error is higher than desired, but is still better than that of typical of calibrations of this sort[19] and has the significant advantage of absolute accuracy afforded by traceable measurement procedures.

ACKNOWLEDGMENTS

We thank Mr. Jonathan Mulholland for his assistance with some of the preliminary experiments. Mr. Mulholland was supported through the NIST/NSF Summer Undergraduate Research Fellowship.

REFERENCES

1. W.C. Oliver and G.M. Pharr, J. Mater. Res. **7,** 1564 (1992).
2. T.W. Wu, A.L. Shull, and R. Berriche, Surf. Coat. Technol. **47,** 696 (1991).
3. M.D. Kriese, D.A. Boismier, N.R. Moody, and W.W. Gerberich, Eng. Fract. Mech. **61,** 1 (1998).
4. S. Umemura, S. Hirono, A. Yasuko, and R. Kaneko, IEICE Trans. Electron. **E81-C,** 337 (1998).
5. M. Grandbois, M. Beyer, M. Rief, H. Clausen-Schaumann, and H. Gaub, Science, **283,** 1727 (1999).
6. ISO group TC 164/SC 3/WG 1 and ASTM E28.06.11, Metallic Materials—Instrumented Indentation Test for Hardness and Materials Parameters, ISO 14577-1, 2, and 3 (International Organization for Standardization, 2002).
7. J. Lawall and E. Kessler, Rev. Sci. Inst. **71,** 2669 (2000).
8. Z.J. Jabbour and S.L. Yaniv, Journal of Research of the National Institute of Standards and Technology **106,** 25 (2001).
9. E.R. Williams, R.L. Steiner, D.B. Newell, and P.T. Olsen, Phys. Rev. Lett. **81,** 2404 (1998).
10. T. Funck and V. Sienknecht, IEEE Transactions on Instrumentation and Measurement **40,** 158 (1991).
11. D.B. Newell, J.A. Kramar, J.R. Pratt, D.T. Smith, and E.R. Williams, IEEE Transactions on Instrumentation and Measurement **52,** 508 (2003).
12. J.A. Kramar, D.B. Newell, J.R. Pratt, in *Proceedings of the Joint International Conference IMEKO TC3/TC5/TC20*, VDI-Berichte 1685, (VDI Verlag, Düsseldorf, Germany) pp. 71–76.
13. J.R. Pratt, D.B. Newell, and J.A. Kramar, in *Proceedings of the joint international conference IMEKO TC3/TC5/TC20*, VDI-Berichte 1685, (VDI Verlag, Düsseldorf, Germany) pp. 77–82.
14. T.J. Sneden and W.A. Ducker, Langmuir **10,** 1003 (1994).
15. C.T. Gibson, G.S. Watson, and S. Myhra, Nanotechnology **7,** 259 (1996).
16. M. Tortonese and M. Kirk, Characterization of Application Specific Probes for SPMs, SPIE 3009 (Society of Photo-Optical Instrumentation Engineers, Bellingham, WA, 1997), p. 53.
17. W. Hoffman, S. Loheide, T. Kleine-Besten, U. Brand, and A. Schlachetzki, 2000, Methods of Characterizing Micro Mechanical Beams and Its Calibration for the Application in Micro Force Measurement Systems, Proc. EXPO World Microtech congress (MICRO.tec 2000), **2,** Hannover, Germany, VDE, pp. 819–823.
18. D. Sarid, *Scanning Force Microscopy* (Oxford University Press, New York, 1994).
19. J.D. Holbery, V.L. Eden, M. Sarikaya, and R.M. Fischer, Rev. Sci. Instrum. **71,** 3769 (2000).
20. L.P. Howard and J. Fu, Accurate Force Measurements for Miniature Mechanical Systems: A Review of Progress, SPIE 3225 (Society of Photo-Optical Instrumentation Engineers, Bellingham, WA, 1997) pp. 2–11.
21. M. Tortonese, R.C. Barrett, and C.F. Quate, Appl. Phys. Lett. **62,** 834 (1993).
22. J. Harley, 2000, Ph.D. Thesis, Stanford University, Palo Alto, CA (2000).
23. C. Smith, Phys. Rev. **94,** 42 (1954).
24. B. Du, M.R. VanLandingham, Q. Zhang, and H. Tianbai, J. Mater. Res. **16,** 1487 (2001).
25. C.T. Gibson, G.S. Watson, and S. Myhra, Scanning, **19,** 564 (1997).

Downloaded from http://www.cambridge.org/core. the NIST Virtual Library (NVL), on 27 Sep 2016 at 19:16:31, subject to the Cambridge Core terms of use, available at http://www.cambridge.org/core/terms. http://dx.doi.org/10.1557/jmr.2004.19.1.366